Thermal-Hydraulic Analysis of the EU DEMO Helium-Cooled Pebble Bed Breeding Blanket Using the GETTHEM Code

Thermal-hydraulic analysis of the EU DEMO Helium-Cooled Pebble Bed Breeding Blanket using the GETTHEM code

Antonio Froio, Fabio Cismondi, Laura Savoldi, *Member, IEEE*, and Roberto Zanino, *Senior Member, IEEE*

***Abstract*—The GEneral Tokamak THErmal-hydraulic Model – GETTHEM has been updated to the most recent version of the EU DEMO Helium-Cooled Pebble Bed (HCPB) Breeding Blanket (BB) design. The GETTHEM results are first benchmarked in a controlled case against the results of 3D Computational Fluid-Dynamics computations, showing an acceptable accuracy despite the inherent simplifications in the GETTHEM model. GETTHEM is then applied to the evaluation of the poloidal hot-spot temperature distribution in an entire BB segment, showing that the maximum temperature in the EUROFER structures overcomes the design limit of 550 °C by more than 50 °C in some Blanket Modules. A possible mitigation strategy is then proposed and analyzed, based on the idea of cooling the First Wall in parallel with the breeding zone, showing that this solution would allow having the EUROFER in its working temperature range in the entire segment, although at the expense of a larger pressure drop.**

***Index Terms*—nuclear fusion, EU DEMO, HCPB, First Wall, EUROFER, GETTHEM**

I. Introduction

THE EU DEMO reactor, see Fig. 1, currently in the pre-conceptual design phase coordinated by the EUROfusion consortium, should produce net electrical energy from nuclear fusion by the 2050s [3].

Within this framework, a system-level code, the GEneral Tokamak THErmal-hydraulic Model (GETTHEM), is under development at Politecnico di Torino since 2015, with the support of the EUROfusion Programme Management Unit.

The main aim of the code, developed in a modular fashion using the Modelica® object-oriented modeling language, is the fast and reasonably accurate simulation of thermal-hydraulic transients of the entire Primary Heat Transfer System (PHTS) – a need, which is especially relevant in this phase of the project.

GETTHEM currently comprises models for the cooling loops of the Helium-Cooled Pebble Bed (HCPB) [4] and Water-Cooled Lithium-Lead (WCLL) [5] Breeding Blanket (BB) concepts and has been already successfully applied to the optimization of the coolant flow in the HCPB BB normal operation [6], as well as verified/benchmarked against Computational Fluid-Dynamics (CFD) simulations of the WCLL BB [7]. Moreover, GETTHEM is being applied to the safety analysis of an in-vessel Loss-Of-Coolant Accident, for both HCPB [8] and WCLL [9].

In the present work, the HCPB module of the code, updated to the most recent HCPB design, is applied to analyze the hot-spot temperature in the solid structures of the BB. The paper is organized as follows: in the first part, the current design of the HCPB BB is briefly introduced, the main features of the GETTHEM code are recalled and the thermal-hydraulic drivers are defined; in the second part, after presenting a benchmark of the model against a 3D CFD simulation in a controlled case, the temperature distribution in the EUROFER structures of an entire BB segment is presented, identifying the most critical points of the BB; finally, the tool is used to check the effect of a possible design change, that could improve the outcome by decoupling the FW in the most loaded components.

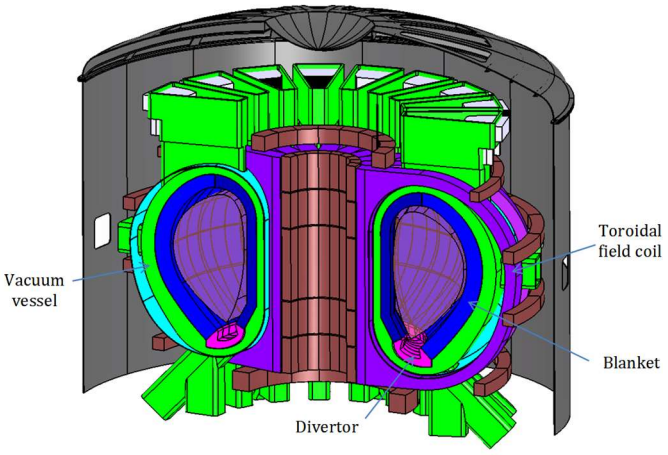

Fig. 1. A sketch of the 2015 baseline design of the EU DEMO1 tokamak [1], [2], showing the main components. The outermost (grey) component, the cryostat, has ~ 40 m diameter and is ~ 30 m tall.

Manuscript received November 13, 2017

This work has been carried out within the framework of the EUROfusion Consortium and has received funding from the Euratom research and training programme 2014-2018 under grant agreement No. 633053. The views and opinions expressed herein do not necessarily reflect those of the European Commission.

A. Froio (antonio.froio@polito.it), L. Savoldi (laura.savoldi@polito.it), and R. Zanino (roberto.zanino@polito.it) are with the NEMO group, Dipartimento Energia, Politecnico di Torino, 10129 Torino, Italy.

F. Cismondi (Fabio.Cismondi@euro-fusion.org) is with the PPPT Department, EUROfusion Consortium, 85748 Garching bei München, Germany.

II. The 2015 HCPB BB Design

In the 2015 baseline design [1], the EU DEMO tokamak is subdivided in 18 identical sectors in the toroidal direction; each sector contains three outboard (OB) and two inboard (IB) BB segments. Four possible BB concepts are being explored: the aforementioned HCPB (object of this study and responsibility of KIT, Germany) and WCLL (responsibility of ENEA, Italy), plus the Helium-Cooled Lithium-Lead (responsibility of CEA, France) [10] and the Dual-Cooled Lithium-Lead (responsibility of CIEMAT, Spain) [11].

Each BB segment contains several Blanket Modules (BMs), in varying number depending on the blanket concept; for the HCPB, 7 BMs are foreseen both for the IB and the OB segments, see Fig. 2.

A cross section of a HCPB Blanket Module is reported in Fig. 3 and Fig. 4. The Breeding Zone (BZ) is composed of a tritium-breeding material, in the form of Li_4SiO_4 pebbles, and a neutron-multiplying material, made of Be pebbles. The Blanket Module is arranged as a series of poloidally-stacked beds alternating the two materials, separated by metallic Cooling Plates (CPs) providing both a pathway for the coolant and a stiffening structure.

The HCPB is cooled by helium at 8 MPa, with nominal inlet and outlet temperatures of 300 °C and 500 °C, respectively, to ensure that the Reduced Activation Ferritic Martensitic steel (EUROFER) of the solid structures is always working inside the allowed temperature range; in particular, the upper limit is identified as 550 °C, to avoid a reduction of the creep strength [14].

The cooling system is divided in two perfectly antisymmetric loops (named "A" and "B"), running in countercurrent. The Primary Heat Transfer System layout foresees six separate circuits to cool three outboard sectors each, and three circuits to cool six inboard sectors each. The cooling loop of each BM, schematized in Fig. 5, is split in two regions, the FW and the BZ, cooled according to the "series" cooling concept. As visible in Fig. 4, in addition to the channels of loops A and B, the CPs contain a third type of channels, which are referred to as "dummy" channels as no coolant flows inside them; all the channels are equally spaced, but the number of dummy channels in between two active channels increase going from the FW to the BSS, in order to have more cooling power close to the plasma.

III. The GETTHEM HCPB BB Cooling System Model

GETTHEM models the thermal-hydraulic transient operation of the HCPB BB cooling system using a 0D/1D approach: for components such as pumps, valves, and manifolds, a 0D transient mass and energy balance is solved, whereas for components such as channels and pipes the 1D mass, momentum and energy balance is solved with the Finite Volume (FV) approach (see [6] for details).

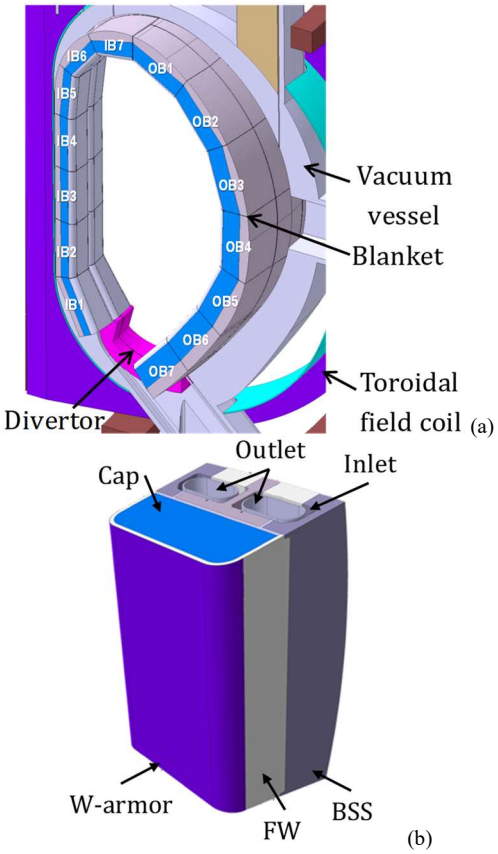

Fig. 2. Blanket segmentation, showing the numbering convention of the HCPB IB1-7 and OB1-7 BMs (adapted from [12] [13]): a) blanket sector; b) BM with back supporting structure (BSS).

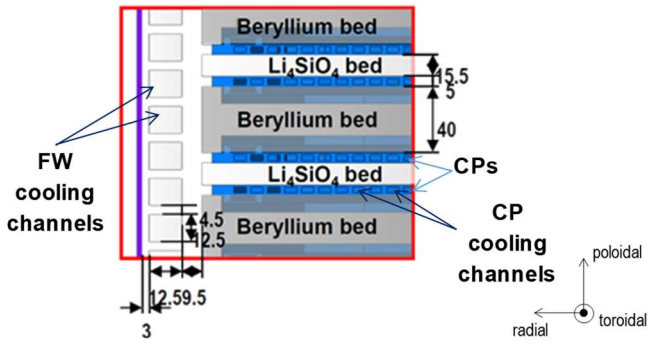

Fig. 3. Radial-poloidal cross section of a HCPB BM, showing the alternate structure of breeder, neutron multiplier and cooling plates (adapted from [4]).

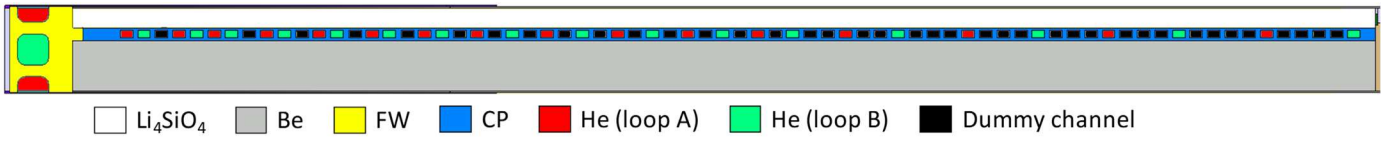

Fig. 4. Radial-poloidal cross section of a HCPB BM, showing the different materials and highlighting the channels of loops A and B, as well as the dummy channels in the CP.

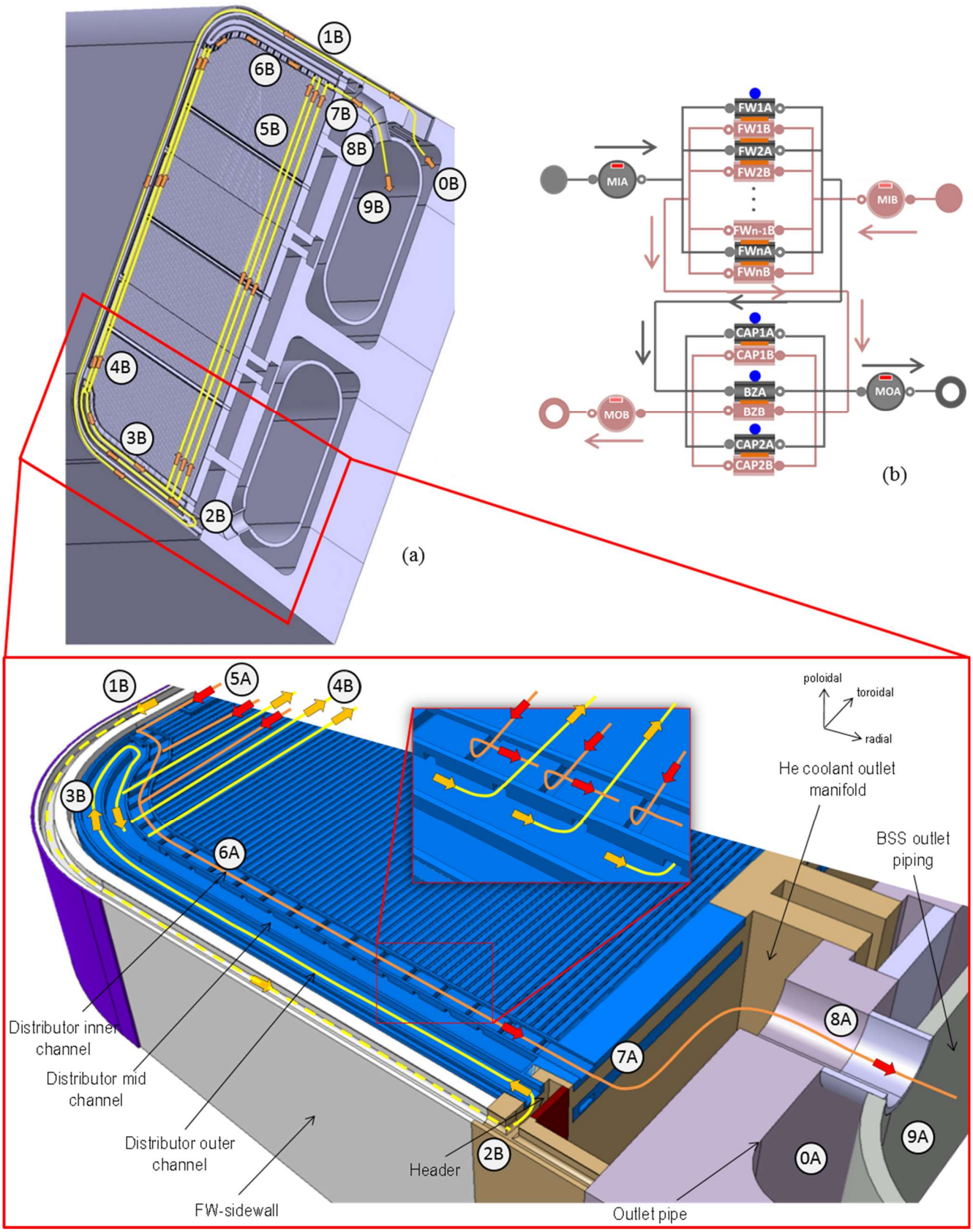

Fig. 5. Scheme (a) and GETTHEM model (b) of the coolant flow path inside a HCPB BM (adapted from [4], [6], [13]). a) The coolant is distributed initially from the manifold in the BSS (bullet 0) to the FW square cooling channels (bullet 1), and it is successively collected and redistributed (bullets 2 and 3, respectively) to the CP rectangular cooling channels (bullets 4 and 5) by a rather complex system of internal manifolds, before being collected again in a manifold inside the CP at first (bullet 6) and in a BM-wide manifold (bullet 7), which finally delivers the hot coolant to the outlet manifold inside the BSS (bullets 8 and 9). The dark-colored lines and arrows refer to loop A, whereas the light-colored ones refer to loop B. b) The BSS manifolds ("M" objects) are modelled as 0D components, distributing the coolant to the FW channels ("FW#" objects), which are in turn connected to the BZ (BZ objects) and to the two BM caps (CAP# objects); the orange rectangles represent the thermal coupling between the two loops. The details of the models of FW channels, CAPs and BZ objects are reported in [6].

The energy conservation in the solid structures is also solved with a simplified model: the EUROFER surrounding each channel is split in two parts, see Fig. 6, and each one is discretized using 1D Finite Volumes in the direction of the flow as the respective channel; each solid volume transfers heat by convection to the adjacent fluid volume and is coupled through a conductive resistance (computed conservatively considering the dummy channel surfaces as adiabatic) with the solid volume belonging to the neighboring active channel (solid volumes *belonging to the same active channel* are assumed to transfer heat only through the helium in the channel [6]). As the number of dummy channels between two active channels varies in the radial direction, as mentioned, two possible cases are found, i.e. when this number is even (or 0) or when it is odd. As the rationale is to split the solid volume in two equal parts, in the first case the two solid volumes are split at the midpoint between two channels (dummy or active), whereas in the latter the two solid volumes are split at the midpoint of the central dummy channel (see Fig. 6).

Since the model is 1D along the flow direction, the solid temperature computed in each volume is averaged in the directions perpendicular to the flow. Notice that this is a quite coarse discretization of the solid structures in the planes orthogonal to the flow direction, compared to what can be done e.g. through CFD. Considering this limitation, a suitable, albeit ad-hoc, post-processing of the GETTHEM results will be described below, which allows to get an estimate of the hot-spot temperature in the structures.

For the model to be fast to execute, some simplifying assumptions had to be made, in view of the very large number of independent cooling channels to be modelled (~1700 per BM in the current design).

In particular, we assume that the helium can be treated as an ideal gas, which is reasonable considering the temperatures and pressure of interest. The thermophysical properties of EUROFER are assumed to be independent of temperature, which introduces a maximum (input) error within ±0.6 %, ±18 %, and ±5 % on EUROFER density, specific heat and thermal conductivity, respectively, and an error within ±0.3 %, ±8 % and ±3 % on average; also the heat transfer coefficient (HTC) between solid and fluid is assumed constant (although it can be different among the BMs) and equal to the values computed in [13] using the Gnielinski correlation [15]. The input error due to all these simplifications, however, translates into an error on the output always below 3 %, both in terms of temperatures (coolant and structures) and of transient duration. Finally, the heat transfer between First Wall and Cooling Plates, as well as between neighboring cooling plates, is neglected.

Moreover, the 2 mm tungsten armor on the FW is (currently) neglected in the model; as shown in [16], however, this term affects the maximum temperatures by less than 1 %. Although the Li_4SiO_4 and Be pebble bed could be easily added to the model, they are not considered in this work, as, at the expense of a rather more complex (and computationally heavy) model, they would only affect the duration of the transient and not the steady-state EUROFER temperature value, which is the main objective of this study as justified in Section IV below. Finally, GETTHEM currently models only the in-vessel components, i.e. the Blanket Modules and the manifolds in the Back Supporting Structure (the latter using a 0D approach [6]); the ex-vessel part of the cooling system is reduced to boundary conditions at the inlet/outlet of the BMs, prescribing the pressure at the inlet and outlet (p_{in} and p_{out}, respectively), and the inlet temperature (T_{in}). Being the BSS modeled as a couple of 0D manifolds, all the BMs share the same inlet and outlet pressure, so that they are in a perfect hydraulic parallel. A schematic representing the model considered for the present work is reported in Fig. 7.

IV. Input Heat Loads

The thermal load input to each BM can be split in two components, i.e. the load to the Breeding Zone and the load to the First Wall.

The poloidal distribution of the load on the BZ is reliably computed by neutronic analyses [13] and reported in Table I and Fig. 8. This heat load is not uniformly distributed in the radial direction, but a radial power peaking factor

$$f_p^Q(r) = \frac{Q(r)}{\overline{Q}} \tag{1}$$

where $Q(r)$ is the radial profile of the power generation (W/m³) and $\overline{Q}$ is the average power generation, is also computed in [13] and applied here. The value of this peaking factor, as a function of the Cooling Plate active channel number, is reported in Fig. 9 (by convention, the channels are numbered starting from the one closest to the plasma).

The loads to the FW are assumed to come only from the plasma (W/m²), in the form of charged particles (ions / electrons) and radiation (photons), i.e. the nuclear load to the FW is neglected here. These loads are used to design the FW shape (in order to minimize the heat flux to the FW), and depend on the plasma equilibrium. Consequently, these heat loads vary according to the plasma conditions.

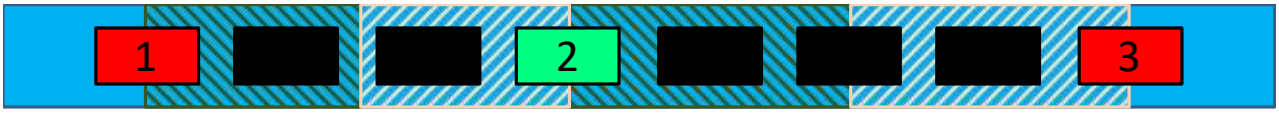

Fig. 6. Cross section of a CP, showing the split of the solid volume between adjacent channels, in the two possible cases: when the number of dummy channels between two active channels is even or 0 (as for channels 1-2), and when it is odd (as for channels 2-3). The color code is the same as Fig. 4.

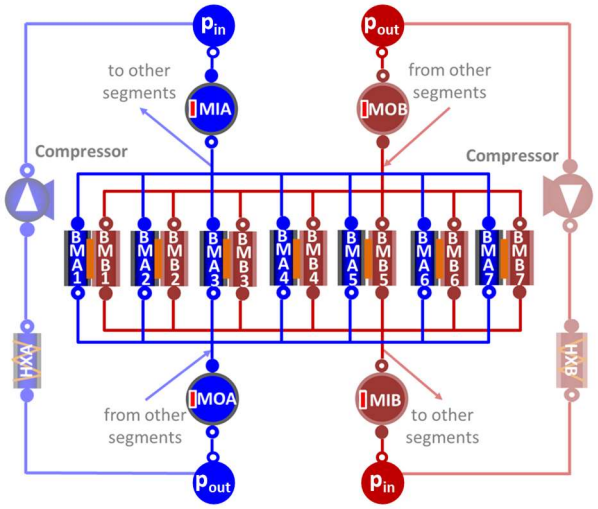

Fig. 7. GETTHEM model of the HCPB cooling system: the ex-vessel components (greyed-out), not yet modelled, are substituted by fixed pressure boundary conditions (represented by the circles p_{in}/p_{out}). MIA/MIB: Inlet Manifold, loop A/B; MOA/MOB: Outlet Manifold, loop A/B.

TABLE I
POLOIDAL DISTRIBUTION OF DESIGN LOADS AND COOLANT MASS FLOW [13]

Module	BZ load (MW)	FW load (MW)	Mass flow rate (kg/s)
OB1	2.52	1.00	3.4
OB2	3.87	1.28	5.0
OB3	4.83	1.40	6.0
OB4	5.06	1.52	6.3
OB5	4.44	1.45	5.7
OB6	3.79	1.31	4.9
OB7	2.84	1.13	3.8
IB1	2.02	1.04	2.9
IB2	2.10	0.967	2.9
IB3	2.60	0.962	3.4
IB4	2.53	0.962	3.4
IB5	2.27	0.802	3.0
IB6	2.89	0.833	3.6
IB7	2.04	1.01	2.9

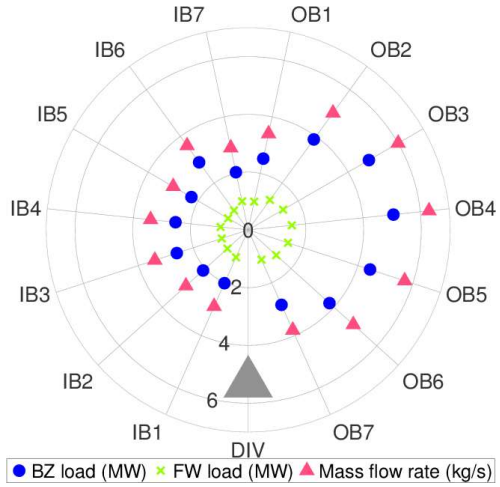

Fig. 8. Poloidal distribution of the heat load to the BZ (blue circles) and FW (green crosses), and of the coolant mass flow rate (pink triangles; DIV = divertor) [13].

The dependency of these loads on the plasma behavior makes them hard to predict accurately, so that, as a first approach, the needed coolant mass flow rate in each BM was evaluated by the design team under the assumption of a uniform heat flux distribution; in particular, a uniform heat flux of 0.5 MW/m² was assumed in [4], which leads to the total power and needed mass flow rate distribution, computed through an energy balance to achieve the desired steady-state target temperature increase, as reported in Table I and Fig. 8.

Finally, steady-state conditions will be assumed throughout our analysis, since the heat loads are constant during the plasma burn phase, and the latter lasts much more (~2 h [17]) than the characteristic times of the helium coolant advection in the channels ($L_{channel}$ / v_{He} ~ 1 m / 10 m/s ~ 0.1 s) and of the thermal transient in the EUROFER structures ((VOL/SURF)$_{EUROFER}^2$ / $\alpha_{EUROFER}$ ~ 50 mm² / 5 mm²/s ~ 10 s), as already shown in [6] and by other authors in [18]. Nevertheless, because of the intrinsically transient nature of the Modelica® language [6], we compute the steady state as the result of ~150 s of transient simulation with constant heat load, starting from an initial uniform "cold" state (i.e., all components at the inlet temperature of 300 °C).

V. GETTHEM-CFD BENCHMARK

A. Comparison of Local EUROFER Temperature Distributions

To have an idea of the reliability of the GETTHEM calculations of the solid temperatures, it is benchmarked here against the 3D conjugate heat transfer CFD study performed by the HCPB design team, which is described in [4] and detailed in [13], [16], [19].

As the CFD study was carried out on a unit slice at the midplane of the Blanket Module (including one and "two halves" of First Wall channels and one Cooling Plate, as shown in Fig. 10), with symmetry conditions on the top and bottom surfaces, it cannot consider boundary effects, i.e., it is a representation of a BM with infinite length in the poloidal direction; moreover, it was applied to the outboard equatorial BM (OB4), which is the only one whose detailed design is presently available. For this reason, the CFD results are compared with the GETTHEM results computed in a CP at the OB4 midplane, in order to reduce as much as possible the boundary effects.

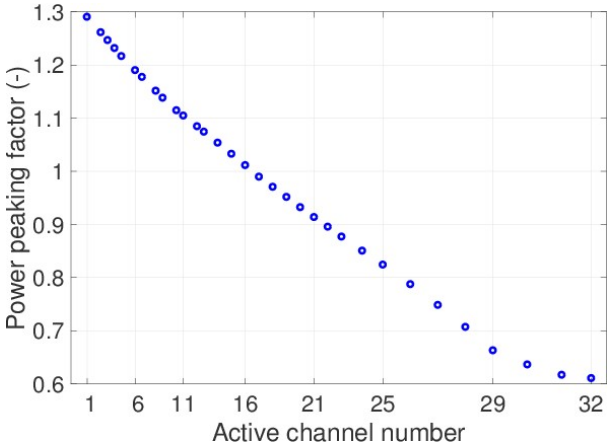

Fig. 9. Radial distribution of the power peaking factor for the BZ heat load [13].

In addition, as mentioned above, the Be and Li_4SiO_4 layers are not modelled in GETTHEM, as well as the purge gas; in particular, the first ones do not affect the steady-state temperature, as already discussed, whereas the latter was shown in [19] to have negligible effects.

We recall that the radial-poloidal discretization of the solid structures in the Breeding Zone adopted by GETTHEM is very coarse: to have a fair comparison, the CFD results are here postprocessed by computing the volume-averaged temperature in the EUROFER around each CP cooling channel, and the outcome is compared with the average solid temperature around each channel computed by GETTHEM, see Fig. 11; the error bars on the CFD curve refer to an estimated maximum error of 5 K as reported in [13], whereas those on the GETTHEM curve are computed accounting for the aforementioned estimated maximum error of 3 %.

The most evident difference between the two curves is that the CFD temperature distribution is non-monotonic (despite the monotonic power generation profile), whereas the GETTHEM one is monotonically decreasing from the FW to the BSS. The non-monotonic behavior of the CFD curve is due to multiple reasons: the first local minimum (channels 5-6) is found in correspondence with the purge gas ducts, which provide an additional heat sink (as mentioned above and confirmed here, this effect is anyway small). On the other hand, the local maximum found in channels 14-15 is explained looking at the mass flow rate distribution among the cooling channels (reported also in Fig. 11), which has a minimum in those channels, resulting in a reduction of the cooling power. Finally, the local maximum found in channels 25-26 coincides with a rarefaction of the active cooling channels, with the number of dummy channels between active ones quickly rising from one to three in that region, see Fig. 4, causing that region to be partly undercooled.

The radial distribution of the temperature profile computed by GETTHEM is, instead, monotonically decreasing from the FW towards the BSS, following the power generation profile. The first CFD minimum, caused by the purge gas ducts, cannot be present in the GETTHEM results, as the purge gas ducts are neglected in the GETTHEM model. The maximum in channel 15, due to the mass flow rate distribution, is also not present, despite the fact that GETTHEM computes the same mass flow rate distribution as the CFD; this could be explained considering that in the CFD model the effect of a mass flow rate reduction (with constant heat load) on the solid temperature is twofold, as it makes the coolant temperature increase more, but also reduces the heat transfer coefficient between solid and fluid, further increasing the solid temperature. This second effect cannot however be seen in the GETTHEM results, as the HTC between solid and fluid is assumed constant, as mentioned. Finally, the third feature identified above, namely the maximum in channel 26, cannot be found in GETTHEM as well, since the thermal resistance used to couple adjacent channels only considers locally the EUROFER a 0D volume around the channels; this also explains why the discrepancy between the two models is larger from this point onwards: the larger presence of dummy channels, in fact, makes the lumped-parameter approach used by GETTHEM a worse approximation of the 3D heat conduction.

Despite these differences, the relative discrepancy between the two models is always smaller than 10 %, with the average discrepancy below 5 %. Moreover, this error affects more the region where the temperature is expected to be lower, as mentioned.

B. EUROFER hot-spot temperature estimates

The GETTHEM results can be postprocessed to reconstruct also the hot-spot solid temperature, by applying a peaking factor (different for the two regions, First Wall and Breeding Zone). The value of this peaking factor is determined independently of the GETTHEM results by looking at the detailed temperature distribution computed through the aforementioned 3D conjugate heat transfer CFD study. The peaking factor $f_{p,R}^{CFD}$, where subscript *R* refers to the different regions (FW or BZ), is defined as

$$f_{p,R}^{CFD} = \frac{T_{\max,R}^{CFD} - T_{He,in}}{T_{ave,R}^{CFD} - T_{He,in}} \tag{2}$$

where $T_{\max,R}^{CFD}$ is the maximum EUROFER temperature in region *R* in the slice computed by CFD, $T_{ave,R}^{CFD}$ is the volume-averaged EUROFER temperature in region *R* in the slice computed by CFD and $T_{\mathrm{He,in}}$ is the helium inlet temperature of 300 °C.

In the postprocessing phase, this peaking factor is then applied to the GETTHEM results, according to (3):

$$T_{\max,R}^{GETTHEM} = T_{He,in} + f_{p,R}^{CFD}\left(T_{ave,R}^{GETTHEM} - T_{He,in}\right) \tag{3}$$

In order to be consistent with the definition of the peaking factor, $T_{ave,R}^{GETTHEM}$ is the volume-averaged temperature in one FW cooling channel or one Cooling Plate in GETTHEM, which are equivalent to the CFD unit slice. A flow chart summarizing the postprocessing needed to obtain the hot-spot temperature is reported in Fig. 12.

The value of the peaking factor may differ from BM to BM in view of the different dimensions of the structures; however, as no detailed dimensioning of BMs other than OB4 was ever performed, no additional information could be exploited, and, for the sake of simplicity, it is here assumed that the peaking factor computed for OB4 can be applied as-is to all BMs.

The hot-spot temperatures in the two regions, obtained by postprocessing the GETTHEM results, are compared in Table II to the maximum EUROFER temperatures computed by CFD. An excellent agreement between the GETTHEM and CFD models is noticed, with an error below 1 % on the two solid temperatures.

Table II highlights also the accuracy of GETTHEM as far as the thermal-hydraulics of the cooling channels is concerned, despite the model simplifications.

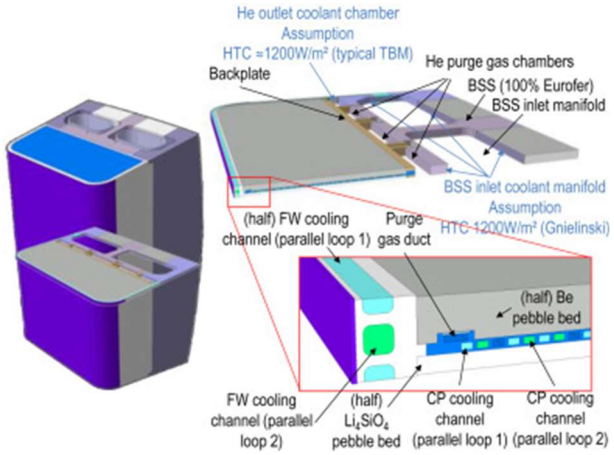

Fig. 10. CFD computational domain ("unit slice", reproduced from [4]).

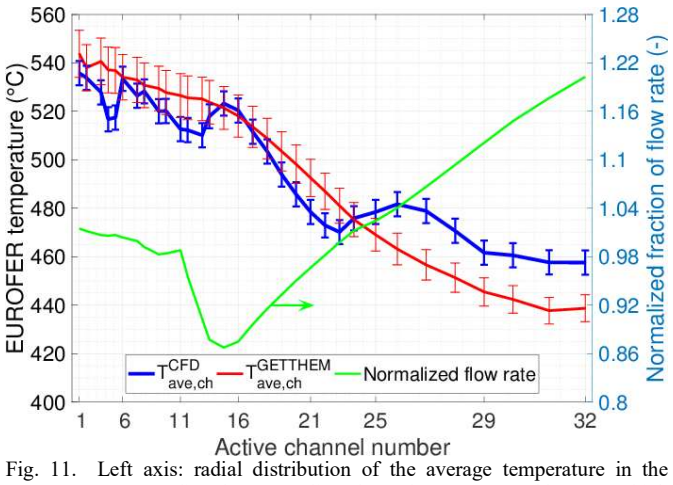

Fig. 11. Left axis: radial distribution of the average temperature in the EUROFER surrounding the CP cooling channels, as computed by CFD (thick blue line) and GETTHEM (thin red line); right axis: radial distribution of the He mass flow rate (normalized to the average) among the CP cooling channels (GETTHEM and CFD curves are superimposed, hence only one is shown).

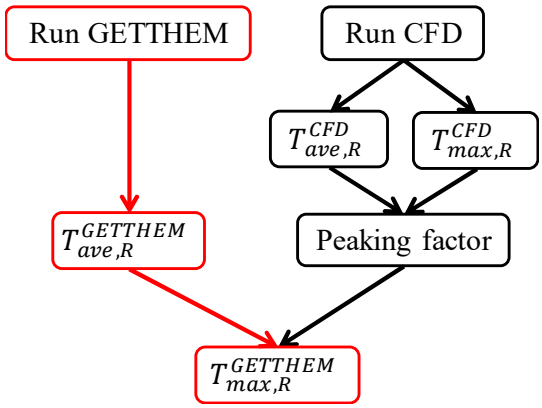

Fig. 12. Flow chart representing the steps needed to compute the hot-spot EUROFER temperature from GETTHEM results.

TABLE II
BENCHMARK OF GETTHEM CALCULATIONS AGAINST 3D CFD

	GETTHEM	CFD [13], [19]	Discrepancy
$T_{He,out}$	466 °C	471.2 °C	3 %
$T_{max,EUROFER,FW}$	515 °C	514.4 °C	0.3 %
$T_{max,EUROFER,BZ}$	554 °C	556.6 °C	1 %

The discrepancy is computed with respect to the temperature increase.

It should also be stressed that, even if the temperature limit is slightly overcome, the hot-spot is located in the BZ region, in regions where the mechanical stresses are relatively small [13].

As an example of the EUROFER temperature distribution computed by GETTHEM on the FW surface of the BMs, the OB4 case is reported in Fig. 13. From this figure, it is evident how the hot-spot is typically located downstream the boundary channels (i.e., the uppermost and lowermost in the poloidal direction), and, by conduction, also in the neighboring ones: in fact, in these two channels the beneficial effect of the alternating countercurrent channel structure is half of that of the "bulk" channels, as the heat transfer occurs between two channels instead of three. As a consequence, the FW hot-spot temperature computed by GETTHEM for this BM is higher than that predicted by CFD, which, on the other hand, is very close to GETTHEM result at the midplane, as reported above.

This boundary effect is also causing the "band" structure, clearly visible in the 2D temperature map of the FW: in fact, the channels in the "bulk" have a perfect symmetry in the toroidal direction, whereas the channels close to the boundaries in poloidal direction do not feel the "averaging" effect of the countercurrent structure, reaching a higher temperature downstream and a lower temperature upstream. Since the first and last channels run in opposite directions, by conduction this "diagonal" band is formed in the temperature distribution.

VI. RESULTS OF GETTHEM WHOLE SEGMENT ANALYSIS

GETTEHM is then applied to an entire BB segment, including both inboard and outboard Blanket Modules; the results, in terms of poloidal hot-spot temperature distribution, are reported in Fig. 14, where the temperature limit of 550 °C is also shown. The peak temperature is higher than the limit, not only in the OB4 Breeding Zone (as expected from the CFD analyses), but in all the BMs, with the most critical point being the IB1, where the FW temperature reaches almost 650 °C. The only other modules to reach temperatures above 600 °C are IB2 and OB1. In all the other BMs, the situation is less critical, with the hot-spot temperature overcoming the limit by few degrees in the OB and by few tens of degrees in the IB.

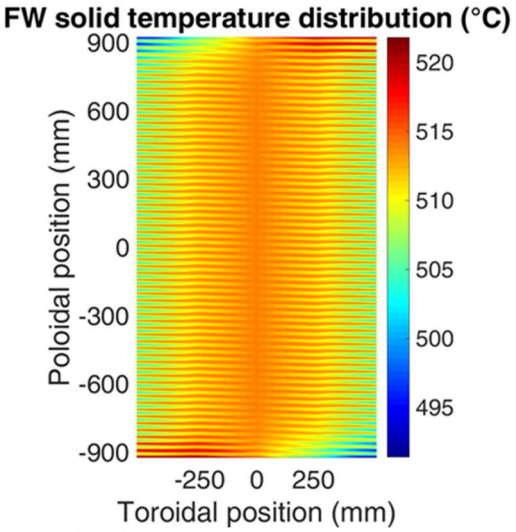

Fig. 13. Map of the solid temperature on the FW surface of the OB4 BM.

It is important to note how BMs with similar loads (and, consequently, mass flow rates) may show different behaviors, as for instance IB1 and IB7, where the difference in the input heat load is ~1 % but the difference on the hot-spot temperature is ~17 % (~50 °C). To understand this difference, it is necessary to consider that the number of FW channels and CPs in the BMs is determined as a function of the BM dimensions [4], i.e. regardless of the mass flow rate of coolant that should flow therein. So, even if all the FW channels and CPs in the BB are identical from the geometrical point of view, the mass flow in each of the cooling channels may vary (even significantly: for instance, the design mass flow rate in a FW channel of the OB4 is 51 g/s, whereas it is only 25 g/s in a IB1 FW channel [13]). Necessarily, this implies reduced coolant speeds, which, in turn, translates in a reduced heat transfer coefficients and related cooling capability. In the above-mentioned IB1 and IB7 (112 and 88 FW cooling channels, 56 and 44 CPs, respectively), the relative difference between the HTCs is ~21 % [13], explaining the difference found in the hot-spot temperature. This shows that the cause of the EUROFER overheating is due to insufficient cooling capabilities of some BMs. Since the rationale for the mass flow repartition between modules cannot change, as it would affect the coolant temperature at the inlet of the steam generator, the results computed here call for a different design of the cooling channels in such BMs with, e.g., heat transfer promoters, which could help in increasing the cooling capability in the weak channels. The analysis of that alternative is, however, beyond the scope of the present paper.

In addition, it is evident from this figure that all the BMs that reach overall maximum temperature values close to or above 600 °C (IB1-5, IB7, OB1 and OB7) have the hot-spot located on the FW, whereas the BMs with temperatures closer to the limit have the hot-spot in the BZ, with FW temperatures often below 550 °C. A "parallel" cooling concept could help to mitigate the overheating in some modules and to keep the entire segment in a safe state by cooling the FW and the BZ separately, as reported in Fig. 15 [12]: in this case, in fact, only the BZ cooling system would provide heat to the steam generator, and the mass flow rate in the FW cooling loop would become a free parameter (as the outlet temperature of this loop will not be a design parameter). The main drawback of that solution is however that the heat deposited on the FW could not be (directly) exploited to produce energy in the Power Conversion System (PCS), although it may still be used e.g. to preheat the water in the PCS, before it enters the steam generator.

GETTHEM is applied here to compare the cooling performances of these two different options, exploiting the parallel cooling strategy on the BMs which showed a hot-spot temperature close to or higher than 600 °C.

The mass flow rate to these BMs *in the BZ circuit* can now be reduced with respect to the value reported in Table I, which was determined in order to remove the power deposited in both BZ and FW, while keeping of course the helium outlet temperature fixed to the design value. Hence, the values of mass flow rate for these BMs in the BZ circuit are computed by scaling the relevant value in Table I with respect to the BZ-only power generation, reported again in Table I. The result is reported in Table III.

On the other hand, as the mass flow rate to the FW of these BMs is now a free parameter, it can be easily determined by GETTHEM analysis, varying the mass flow rate until the FW hot-spot temperature is reduced below the limit. Also in this case the result is reported in Table III.

When considering the parallel cooling option, the differences are necessarily found only in the "parallelized" BMs; in these modules, in fact, the hot-spot temperature is dramatically reduced, reaching values close to those found in the BMs with the series option, as visible in Fig. 16.

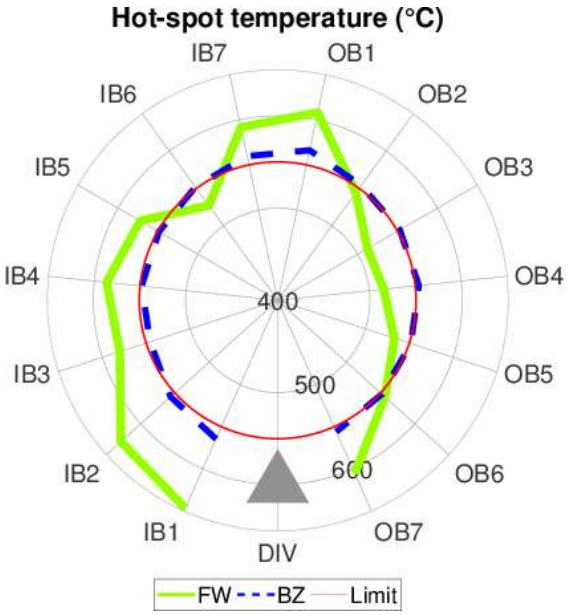

Fig. 14. Peak EUROFER temperature in a HCPB segment, in the FW (green solid line) and BZ (blue dashed line) regions. The thin, pink, solid line represents the operational upper limit of 550 °C.

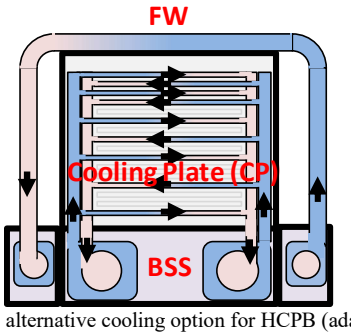

Fig. 15. "Parallel" alternative cooling option for HCPB (adapted from [12]).

TABLE III
COOLANT MASS FLOW RATE IN THE BMS WHERE THE PARALLEL COOLING OPTION IS ADOPTED

BM	BZ mass flow (kg/s)	FW mass flow (kg/s)
OB1	2.4	8.2
OB7	2.7	8.9
IB1	1.9	7.0
IB2	2.0	7.0
IB3	2.5	8.2
IB4	2.5	8.2
IB5	2.2	8.0
IB7	1.9	7.0

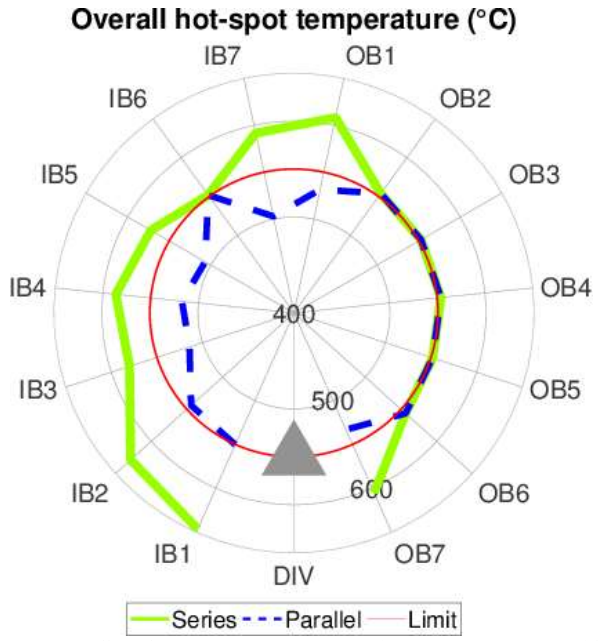

Fig. 16. Overall peak EUROFER temperature in a HCPB segment, with the series (green solid line) and parallel (blue dashed line) cooling options. The thin, pink, solid line represents the operational upper limit of 550 °C.

As a drawback of this solution, the mass flow rate needed in the FW to achieve this result is larger (up to ~2.5×) than the design one, causing the pressure drop in these portions of the FW to reach 3 bar (in contrast with the 2 bar of the series option, as reported in [4] and also computed by GETTHEM). Nevertheless, this change in the cooling system layout is not expected to affect dramatically the overall efficiency of the plant: the dedicated FW loop, in fact, would require ~100 MW of additional pumping power (this is a rough estimate, as no detailed design of this loop is available), while the pumping power in the BZ loop would be reduced by ~20 MW (as a consequence of the reduction of the total mass flow rate). Separated loops for the FW and the BZ could also benefit of a better optimized thermal-hydraulic design with lower pressure drops compared to the same FW and BZ connected in series. Overall, with a first estimate without optimization, the increase of the pumping power could still be acceptable, passing from the currently estimated 150 MW [20] to ~230 MW.

The present analysis has been performed under the assumption that the parallel-cooled FW shares the same hydraulic design of the series-cooled FW; indeed, the th ermal-hydraulics of a parallel FW was not designed yet, and hence it should be possible to further reduce the maximum temperature in the FW without increasing the mass flow rate: in this case, in fact, the FW would become a totally independent component, which could be redesigned in order to withstand such higher heat fluxes (we have not considered the adoption of suitable heat transfer promoters, already under investigation [21], or of the "half-monoblock FW" design proposed by the HCPB design team [22]). Note that the use of heat transfer promoters, such as those analyzed in [21], in the "series" cooling option could actually yield the same result of the parallel option: this would still lead to an increased pressure drop (up to 2.8× [21]), but without increasing the mass flow rate, limiting the increase in the compression power. Eventually, the different solutions could also be mixed, combining half-monoblock FW, heat transfer promoters and parallel FW [22].

VII. Conclusions and Perspective

The GETTHEM system-level code, under development at Politecnico di Torino with the support of EUROfusion, has been applied here to analyze the hot-spot temperature in the EUROFER structures of a whole segment of the HCPB Breeding Blanket.

The model capability to compute the temperature in the solid materials has been benchmarked against the results obtained by other authors through a CFD analysis of a small portion of the GETTHEM domain. Despite the simplifications in the GETTHEM model, the benchmark showed that the discrepancy is reasonable, in view of the different scopes of the two models, particularly considering that the largest error is found in the region with lower temperature. In fact, when looking at the hot-spot temperatures at the midplane, the GETTHEM results are in excellent agreement with the CFD results.

GETTHEM has been then applied to estimate the temperature distribution in the EUROFER in a BB segment. Since in some of the Blanket Modules the temperature overcame the limit of 550 °C by more than 50 °C, the effect of one of the possible alternative cooling options, where the First Wall is cooled in parallel to the Breeding Zone, has been analyzed: it has been shown that this option allows keeping the EUROFER temperature within its working range, at the expenses of an increase in the total pumping power that appears acceptable and has to be quantified once the design of the separated FW and BZ loops will be available.

In perspective, the model will be extended to include the ex-vessel components of the Primary Heat Transfer System (and eventually the Power Conversion System), allowing to analyze the effect of different scenarios (heat loads, cooling concepts, …) on the overall performance of the power plant. Moreover, the possibility to have a water-cooled FW in parallel with a helium-cooled BZ will be added to the model. Finally, a benchmark of GETTHEM against other system codes, such as RELAP, is envisaged for the future.

Acknowledgment

We thank F. Casella for his continuous advice on the Modelica language, R. Bonifetto for his help on the GETTHEM-CFD benchmark and F. Hernández for helpful discussions on the HCPB BB design.

References

[1] R. Wenninger and G. Federici, "DEMO1 Reference Design – 2015 April ("EU DEMO1 2015")," EFDA_D_2LBJRY, 2015, unpublished.

[2] H. Hurzlmeier and B. Meszaros, "EU DEMO1 2015 – DEMO_TOKAMAK_COMPLEX," EFDA_D_2M9AJJ, 2015, unpublished.

[3] F. Romanelli, P. Barabaschi, D. Borba, G. Federici, L. Horton, R. Neu, D. Stork, and H. Zohm, "Fusion Electricity – A roadmap to the realisation of fusion energy," European Fusion Development Agreement (EFDA), 2012, ISBN 978-3-00-040720-8T.

[4] F. A. Hernández González, P. Pereslavtev, Q. Kang, P. Norajitra, B. Kiss, G. Nádasi, and O. Bitz, "A new HCPB breeding blanket for the EU

DEMO: Evolution, rationale and preliminary performances," *Fus. Eng. Des.*, to be published. DOI: 10.1016/j.fusengdes.2017.02.008.

[5] A. Del Nevo, E. Martelli, P. Agostini, P. Arena, G. Bongiovì, G. Caruso, G. Di Gironimo, P. A. Di Maio, M. Eboli, R. Giammusso, F. Giannetti, A. Giovinazzi, G. Mariano, F. Moro, R. Mozzillo, A. Tassone, D. Rozzia, A. Tarallo, M. Tarantino, M. Utili, and R. Villari, "WCLL breeding blanket design and integration for DEMO 2015: status and perspectives," *Fus. Eng. Des.*, to be published. DOI: 10.1016/j.fusengdes.2017.03.020.

[6] A. Froio, C. Bachmann, F. Cismondi, L. Savoldi, and R. Zanino, "Dynamic thermal-hydraulic modelling of the EU DEMO HCPB breeding blanket cooling loops," *Prog. Nuc. Ene.,* vol. 93, pp. 116-132, Nov. 2016.

[7] A. Froio, F. Casella, F. Cismondi, A. Del Nevo, L. Savoldi, and R. Zanino, "Dynamic thermal-hydraulic modelling of the EU DEMO WCLL breeding blanket cooling loops," *Fus. Eng. Des.*, to be published. DOI: 10.1016/j.fusengdes.2017.01.062.

[8] A. Froio, A. Bertinetti, L. Savoldi, N. Pedroni, S. Ciattaglia, F. Cismondi, and R. Zanino, "Analysis of the VVPSS response to a helium-cooled EU DEMO breeding blanket in-vessel LOCA using the GETTHEM code," in *Safety and Reliability – Theory and Applications, Proc. ESREL27*, Portorož, Slovenia, Jun. 18-22, 2017, pp. 59-66.

[9] A. Froio, A. Bertinetti, S. Ciattaglia, F. Cismondi, L. Savoldi, and R. Zanino, "Modelling an In-Vessel Loss of Coolant Accident in the EU DEMO WCLL Breeding Blanket with the GETTHEM Code," presented at the *13th Int. Symposium on Fusion Nuclear Technology (ISFNT-13)*, Kyoto, Japan, Sep. 25-29, 2017 (submitted to *Fus. Eng. Des.*).

[10] G. Aiello, J. Aubert, N. Jonquères, A. Li Puma, A. Morin, and G. Rampal, "Development of the Helium Cooled Lithium Lead blanket for DEMO," *Fus. Eng. Des.*, Vol. 89, No. 7-8, pp. 1444-1450, Oct. 2014.

[11] D. Rapisarda, I. Fernandez, I. Palermo, M. Gonzalez, C. Moreno, A. Ibarra, and E. Mas de les Valls, "Conceptual Design of the EU-DEMO Dual Coolant Lithium Lead Equatorial Module," *IEEE Trans. Plasma Sci.*, Vol. 44, No. 9, pp.1603-1612, Sep. 2016.

[12] L. V. Boccaccini, G. Aiello, J. Aubert, C. Bachmann, T. Barrett, A. Del Nevo, D. Demange, L. Forest, F. A. Hernández González, P. Norajitra, G. Porempovic, D. Rapisarda, P. Sardain, M. Utili, and L. Vala, "Objectives and status of EUROfusion DEMO blanket studies," *Fus. Eng. Des.*, Vols. 109-111, Part B, pp. 1199-1206, Nov. 2016.

[13] F. A. Hernández González, Q. Kang, B. Kiss, H. Neuberger, P. Norajitra, G. Nadási, P. Pereslavtsev, and C. Zeile, "DDD 2015 for HCPB," EFDA_D_2MRQ4E, 2016, unpublished.

[14] L. V. Boccaccini, L Giancarli, G Janeschitz, S Hermsmeyer, Y Poitevin, A Cardella, and E Diegele, "Materials and design of the European DEMO blankets," *J. Nucl. Mater.*, Vols. 329-333, Part A, pp. 148-155, Aug. 2004.

[15] F. Incropera and D. Dewitt, *Fundamentals of heat and mass transfer*, 6th ed.. Singapore: John Wiley & Sons, 2006, p. 515.

[16] B. Kiss, "Thermo-hydraulic analysis support – Activities in 2016," EFDA_D_2MXRHT, 2017, unpublished.

[17] B. Meszaros, "EU DEMO1 2015 plasma and equilibrium description," EFDA_D_2LJFN7, 2015, unpublished.

[18] G. Zhou, F. A. Hernández González, L. V. Boccaccini, H. Chen, and M. Ye, "Preliminary steady state and transient thermal analysis of the new HCPB blanket for EU DEMO reactor," *Int. J. Hydrogen Energy*, Vol. 41, No. 17, pp. 7047-7052, May 2016.

[19] F. A. Hernández González, Q. Kang, B. Kiss, P. Norajitra, G. Nádasi, P. Pereslavtsev, and C. Zeile, "HCPB Design Report 2015," EFDA_D_2MNBH9, 2016, unpublished.

[20] M. Chantant, "HCPB BB PHTS DDD 2016," EFDA_D_2MF5FV, 2017, unpublished.

[21] S. Ruck and F. Arbeiter, "Thermohydraulics of rib-roughened helium gas running cooling channels for first wall applications," *Fus. Eng. Des.*, Vols. 109-111, Part A, pp. 1035-1040, Nov. 2016.

[22] F. A. Hernández González,, P. Pereslavtev, C. Zeile, G. Zhou, I. Maione, O. Bitz, B. Kiss, G. Nádasi, "HCPB Breeding Blanket design and improvements for 2017," presented at *DEMO BB Design and Analysis Methods Meeting*, Brasimone, Italy, April 19-20, 2017.

Antonio Froio received the B.Sc. in Mechanical Engineering in 2012 from Università della Calabria, Rende (CS), Italy, and the M.Sc. degree in Energy and Nuclear Engineering in 2014 from Politecnico di Torino, Turin, Italy; he received also the M.Sc. in Nuclear Engineering from Politecnico di Milano, Milan, Italy, under a double degree program, and the Alta Scuola Politecnica Diploma from Politecnico di Torino and Politecnico di Milano.

In his M.Sc. thesis, he worked on a simplified model of the cooling system of superconducting magnets for tokamak fusion reactors. He is currently a Ph.D. student in Energetics at Politecnico di Torino from 2014; his activity is focused on the development of the system-level GETTHEM code, for the thermal-hydraulic transient modeling of the Primary Heat Transfer System of tokamak reactors.

Fabio Cismondi graduated as a nuclear engineer at the Polytechnic School of Torino (Italy) and obtained his doctoral degree at CEA Cadarache and University of Toulon and Var (France) in Optics, Image Treatment and Processing.

He worked in CEA Cadarache (France) and Karlsruhe Institute of Technology (KIT, Germany) in the Non-Destructive Examination and design of Plasma Facing Components for Nuclear Fusion devices and in the design and analyses of Test Blanket Modules for ITER experimental reactor and Breeding Blankets for DEMO power plant. He worked in Fusion for Energy in Barcelona (Spain) as Responsible Officer for the procurement of Electron Cyclotron Power Sources for ITER. He is presently working for KIT as part of the Programme Management Unit in Garching (Munich, Germany) as Responsible Officer for the Breeding Blanket and Tritium Cycle work packages and as responsible of In-Vessel Components integration for the European DEMO design.

Laura Savoldi (M'11) received the M.Sc. degree in nuclear engineering and the Ph.D. degree in Energetics from Politecnico di Torino (PoliTo), Italy. She has been Associate Professor of nuclear engineering at Dipartimento Energia, PoliTo, since 2014.

Her research interests are in the development, validation, and application of computational tools for the analysis of thermal-hydraulic transients in superconducting magnets, and in this frame, she developed the 4C code for the analysis of thermal-hydraulic transients in superconducting cables, coils and related cryogenic circuits. She co-authored 140+ papers published in international journals and proceedings of international conferences.

Prof. Savoldi serves as a referee for several international journals and conferences of her field of research, among which IEEE Transactions on Applied Superconductivity and IEEE Transactions on Plasma Science.

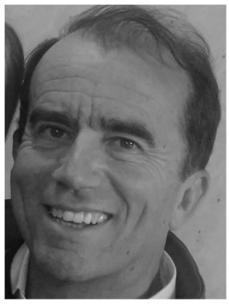

Roberto Zanino (M'11–SM'13) received the M.Sc. degree in nuclear engineering and the Ph.D. degree in energetics from Politecnico di Torino (PoliTo), Italy.

Since 2000, he has been a Professor of nuclear engineering at Dipartimento Energia and since 2011 he is the Head of the graduate studies in Energetics, both at PoliTo. He is the author or coauthor of 150+ papers that appeared in international journals, devoted to computational modeling in fields of relevance for nuclear fusion (superconducting magnets and cryogenics, plasma-wall interactions, high heat flux components, …), nuclear fission (Gen-IV lead-cooled fast reactors) and concentrated solar power (central tower system receivers).

Prof. Zanino is also a member of the American Nuclear Society, of the American Society of Mechanical Engineers and of the International Solar Energy Society.